Ag:TiN-Coated Polyurethane for Dry Biopotential Electrodes: From Polymer Plasma Interface Activation to the First EEG Measurements

Paulo Pedrosa, Patrique Fiedler, Cláudia Lopes, Eduardo Alves, Nuno P. Barradas, Jens Haueisen, Ana V. Machado, Carlos Fonseca, Filipe Vaz*

Several plasma treatments using argon, oxygen, and nitrogen are studied in order to increase the interfacial adhesion of the polyurethane/Ag:TiN system to be used as biopotential electrodes. The optimized plasma treatments conditions (100 W, 15 min, regardless of the gas) promote a steep decrease of the water contact angle values. The observed chemical and topographic alterations translate into excellent polyurethane/Ag:TiN interfacial adhesion of the plasma treated samples. The in-service validation of the proposed Ag:TiN-coated PU multipin electrodes is performed by acquiring EEG signals in parallel with the standard wet Ag/AgCl electrodes. No considerable differences are found in terms of shape, amplitude, and spectral characteristics of the signals when comparing reference wet and dry electrodes.

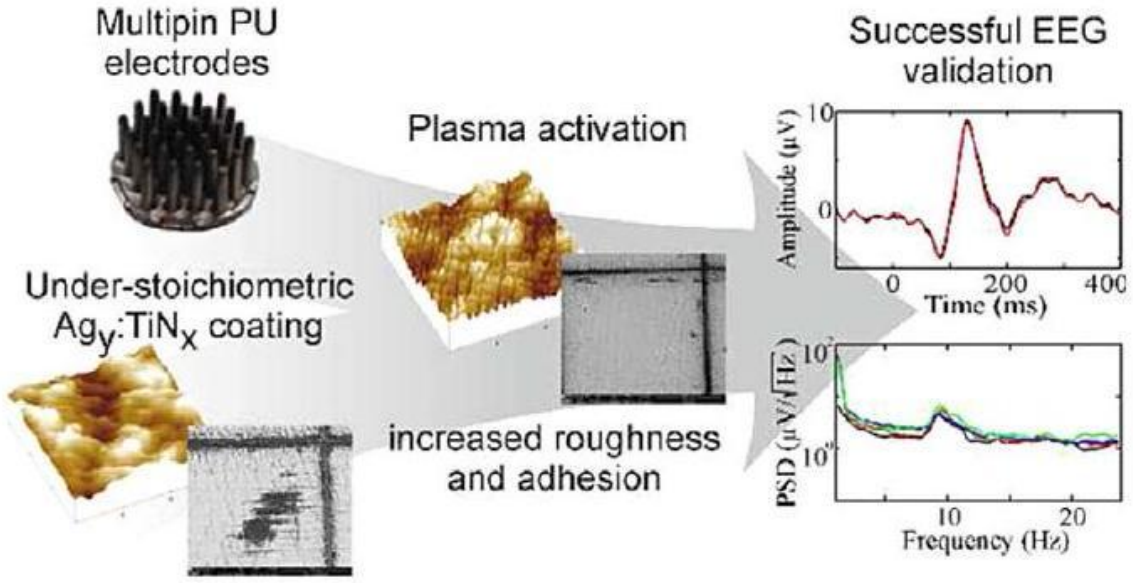

Introduction

The conventional wet silver/silver chloride (Ag/AgCl) electrodes are considered the most suitable for biosignal acquisition [1–3] and are widely used in routine clinical

practices and medical research, such as multichannel electroencephalography (EEG), [4,5] or even brain-computer interfaces. [6–8] They exhibit an essentially non-polarizable, resistive behavior, also displaying an excellent reliability and low, almost frequency-independent skin-contact

impedance values, in the order of few tens of $k\Omega \cdot cm^2$. [2,3] However, the wet Ag/AgCl electrodes suffer from intrinsic technological drawbacks, including difficult, time-consuming, and error-prone skin preparation, [1] as well as limited long-term stability of the gel electrolytes and constant risk of hair damage and skin irritation. [2,3,8]

For the past few years, a new class of dry biopotential electrodes have been studied as potential substitutes for the commercially used wet Ag/AgCl electrodes in applications where, for instance, fast and easy montages are required. This new generation of electrodes does not rely on the application of conductive gels and previous extensive skin preparation, [3,9,10] which translates into higher interfacial impedances. Moreover, incorrect and/or uncomfortable skin contact may arise due to the stiff nature of some of the proposed base materials (aluminium, [3] steel, [11,12] silicon, [13,14] titanium, [15] and polycarbonate [16]), and designspecific conceptual problems (micro-needle electrodes [13,14] and rigid planar plates/disks unable to interfuse the hair layer [15,16]). Hence, in order to reduce some of the referred drawbacks, several authors focused not only on the development of new electrode designs, which allow an effective hair interfusion, [17–20] but also on the use of more compliant base materials, such as textiles [21] and, above all, flexible polymers. [22–25]

Thermoplastic polyurethanes (TPU) have been extensively applied in several fields that range from technical coatings to biomedical applications, [26–28] due to their excellent balance between mechanical properties (high flexibility, dependent on the composition), chemical barrier behavior, soft tact, and biocompatibility, [29,30] thus being appropriate to be used as biopotential electrode base material. Nonetheless, since the present study aims at coating TPU substrates with a previously optimized Ag:TiN thin film system, [31–34] the TPU surface must be suitably activated/functionalized, [35–37] in order to take account of the low surface energy and hydrophobicity (common to most polymers), which may result into poor TPU/Ag:TiN interfacial adhesion. To improve this drawback, a set of low-pressure plasma treatments will be studied, since they are able to tailor important surface characteristics, such as the wettability and topography, [38–40] without compromising the bulk properties of the polymer. Moreover, the low environmental impact promoted by this technique, when compared to other surface activation methods (chemical, thermal, and electrical), has also been reported. [29,41] Depending on the plasma gases and parameters (gas flows, power, pressure, and treatment time), several individual physicochemical effects may be achieved, [42–47] such as surface cleaning (removal of contaminants), etching (roughness promotion), crosslinking, formation of new functional groups, and chain scission (formation of free radicals). The occurrence of these individual effects, or even combination of them (namely increased roughness and formation of new reactive groups), may promote

beneficial effects on the adhesion, by acting as interlock points for active polar groups, [47] thus an increase of the surface wettability is expected. [44,47]

The present work, therefore, investigates, in a first stage, the effect of several argon, [35] oxygen, [30,35,39,48,49] and nitrogen [29] plasma activation treatments, performed with different times and powers on the surface characteristics of the TPU substrates, and subsequent adhesion of the sputtered Ag:TiN film. Then, the plasma activated (using the best treatment time and power for the different gases) novel dry Ag:TiN-coated polyurethane multipin electrodes, which intends to combine the use of a flexible base material (polyurethane, PU) with an optimized design (multipin, MP), were used in several EEG trials in comparison with the wet Ag/AgCl ones. Finally, the quality of the monitored EEG signals was compared in order to assess if the plasmaactivated Ag:TiN-coated PU MP electrodes are suitable to be used as biopotential electrodes.

Experimental Details

Activation and Characterization of the Polyurethane Substrates

The polyester-based thermoplastic polyurethane (TPU) substrates, ref. WHT-1495EC, from Yantai Wanhua Polyurethanes Co., Ltd. were obtained by compression molding in the sheet form. Before all plasma activation treatments, the rectangular polyurethane substrates ($20 \times 30 \times 0.4\ mm^3$) were cleaned with ethanol (96% vol.). A Zepto laboratorysized plasma system from Diener Electronics ($\emptyset = 105$ mm, L = 300 mm, V = 2.6 L, excitation frequency = 40kHz) was used for the plasma activation of the samples, which were placed in a substrate holder at the center of the cylindrical chamber. Several plasma treatments were performed, taking into account the effect of three main parameters: (i) used gas, (ii) plasma treatment time, and (iii) plasma treatment power. The plasma treatment experimental parameters are summarized in Table 1.

Before and immediately after (maximum of 10 min) all activation experiments, the water contact angle (sessile drop method [50,51]) was measured at room temperature, using a OCA 20 unit from Dataphysics, in air-facing polyurethane surfaces. A minimum of six contact angle measurements were performed for each condition. An optimized plasma treatment time (15 min) and power (100 W) were selected from the water contact angle measurements. The chemical bonding characteristics were analyzed by Fourier Transform Infrared Spectroscopy (FTIR) in Attenuated Total Reflectance (ATR) mode, using a Jasco FT/IR 4100 system, equipped with a Specac MkII Golden

Table 1. Plasma treatment parameters.

Parameter	Gas	Power (W)	Time (min)	Pressure $_{base}$ (Pa)	Pressure $_{work}$ (Pa)
Δ Time	Ar	100	2, 5, 10, 15, and 20	3×10^{-3}	8×10^{-3}
	O_2	100	2, 5, 10, 15, and 20	3×10^{-3}	8×10^{-3}

	N_2	100	2, 5, 10, 15, and 20	3×10^{-3}	8×10^{-3}
Δ Power	Ar	100, 75, and 50	15	3×10^{-3}	8×10^{-3}
	O_2	100, 75, and 50	15	3×10^{-3}	8×10^{-3}
	N_2	100, 75, and 50	15	3×10^{-3}	8×10^{-3}

Gate single reflection ZnSe ATR crystal. All ATR-FTIR measurements (64 scans, 4 cm^{-1} nominal resolution) were performed before and immediately after the activation of the samples. In addition, the surface chemistry of the untreated and activated polyurethane samples was also assessed by X-ray Photoelectron Spectroscopy (XPS), performed using a Kratos Axis Ultra spectrometer, equipped with the VISION software for data acquisition and CASAXPS for data analysis. The experiments were carried out with a monochromatic Al K_α x-ray source (1486.7 eV), operating at 15 kV (90 W) in fixed analyzer transmission (FAT) mode, with a pass energy of 40 eV for the regions of interest and 80 eV for the overall surveys. Data acquisition was performed with a pressure lower than 1×10^{-6} Pa, and a charge neutralization system was used. The effect of the electric charge was corrected by the reference of the carbon peak (285 eV). The modeling of the spectra was performed with the CASAXPS program, in which an adjustment of the peaks was done using peak fitting with Gaussian-Lorentzian peak shape and Shirley-type background subtraction. [52]

The surface topography and average roughness (R_a) of the polyurethane substrates was assessed before and after the plasma activation using a Multimode Atomic Force Microscope (AFM) from Digital Instruments using the tapping mode (scan size 3μ m and scan rate 1 Hz). A Nanoscope III controller and Tesp AFM tips from Bruker were also used.

Thin Film Production and Adhesion Characterization

The plasma activated polyurethane substrates were used to deposit Ag:TiN coatings with a N/Ti atomic ratio of 0.7 and 6 at. %Ag by reactive DC magnetron sputtering, in a 60 L custom-made laboratory-sized deposition system. This specific Ag:TiN composition was optimized in previous works by the authors, in order to avoid Ag segregation through the potential formation of Ti_xAg intermetallics. [31–34] The thin films were prepared with the grounded substrate holder positioned at 75 mm from the magnetron and with a 5 rpm rotational speed. A DC current density of 75 $A \cdot m^{-2}$ was applied to the titanium target (99.96 at.% purity/200 $\times$ 100 $\times$ 6 mm^3), containing silver pellets (80 $\times$ 80 mm and 1 mm thick) on its surface distributed symmetrically along the erosion area. The total surface area of the silver pellets ($\sim$ 192 mm^2) was preserved throughout all depositions. A mixed gas atmosphere composed of $Ar + N_2$ was used to generate the plasma. The argon flow was kept constant at 25 sccm in all depositions (partial pressure of 5.4×10^{-1} Pa), while the flow rate of nitrogen fixed at 2 sccm (partial pressure of 4.6×10^{-2} Pa). The working pressure was about 3.8×10^{-1} Pa. A delay time of

5 min was used prior to positioning the sample surface in front of the Ti/Ag target, in order to avoid contamination of the coating resulting from previous depositions, which may have resulted in some target poisoning, as well as to ensure an almost constant deposition temperature during the growth of the films. All depositions were performed for 30 min at room temperature to avoid polymer degradation (together with the grounded condition of substrate holder). Operating conditions are summarized in Table 2.

The atomic composition of the as-deposited samples was measured by Rutherford Backscattering Spectrometry (RBS) using (1.4, 2.3) MeV and (1.4, 2) MeV for the proton and ^{4}He beams, respectively. Three detectors were used. One located at a scattering angle of 140° and two pin-diode detectors located symmetrically to each other, both at 165°. Measurements were made for two sample tilt angles, 0 and 30°. Composition profiles for the as-deposited samples were determined using the NDF software. [53] For the ^{14}N, ^{16}O, and ^{28}Si data, the cross-sections given by Gurbich were used. [54] The area analyzed was about 0.5 × 0.5 mm^2. The uncertainty in the N concentrations is around 5at. %.

The adhesion of the Ag:TiN films to the polyurethane substrates (untreated and plasma treated) was assessed by performing the cross-cut tape test, according to the ASTM D3359-B standard. This test covers procedures for assessing the adhesion of thin films by applying and removing

Table 2. Ag:TiN thin film deposition parameters.

Plasma treatments (performed before all depositions)	Ar 100 W 15 min , $O_2$100 W15 min, $N_2$100 W15 min
Ar (Pa)	5.4×10^{-1}
N_2(Pa)	4.6×10^{-2}
t (min)	30
I ($A \cdot cm^{-2}$)	7.5×10^{-3}
T (°C)	Room temperature
Bias (V)	GND
Pressure $_{work}$ (Pa)	$3.5 - 3.8 \times 10^{-1}$
Pressure $_{base}$ (Pa)	$\sim 10^{-4}$
Area of Ag exposed (mm^2)	192

pressure-sensitive tape over cuts made in the coating. A lattice pattern was manually made in the film (with the cuts reaching the substrate) with an *x*-cutter. Subsequently, the pressure-sensitive tape was applied over the cuts and then removed. The lattice pattern was observed in an electronic microscope before and after removal of the tape and the delamination was classified according to the scale provided in the standard. The SEM/EDS analysis was carried out in a FEI Quanta 400FEG ESEM/EDAX Genesis microscope equipped with X-Ray Microanalysis operating at 15 keV .

EEG Monitoring

In the EEG monitoring tests, a conventional wet Ag/AgCl ring electrode (B10, EASYCAP GmbH, Germany) was placed at frontal position Fp2, while a multipin (MP) test electrode and another wet Ag/AgCl electrode were placed next to each other at occipital position O2. Furthermore, a reference test using two Ag/AgCl electrodes at position O 2 was performed. Prior to electrode placement the skin at each electrode position was cleaned using ethanol and a soft cloth. The Ag/AgCl electrodes were applied in combination with electrolyte gel (Electrogel, EGI Inc., USA), while the MP electrodes (from each plasma activation condition) were used in dry conditions only. Both occipital electrodes were connected to independent bipolar channels of a commercial EEG amplifier (Refa Ext, Advanced Neuro Technologies B.V., The Netherlands), while both channel references were connected to the same frontal electrode at position Fp2. Electrode fixation and adduction was provided by a custommade silicone cap. The MP electrodes were contacted using custom brass mountings. The measurement setup enables simultaneous recording of independent EEG signals. Hence, a direct comparison of the acquired signals using conventional and MP electrodes is possible. Resting-state EEG, alpha activity, and eye-blinking artifacts were monitored
during the in-vivo tests. Also, a pattern reversal visual evoked potential (VEP) was recorded according to ISCEV (International Society for Clinical Electrophysiology of Vision) standards consisting of 300 trials. The three different MP electrodes (activated with argon, nitrogen, and oxygen) and the reference Ag/AgCl electrode were tested in three individual tests per material on three volunteers (two male, one female), resulting in an overall number of 12 test sequences per volunteer. Finally, the simultaneously recorded signals of the wet (w) and dry (d) electrodes were compared by means of the Root Mean Square Deviation (RMSD), the Spearman's rank correlation (CORR) as well as the Welch estimation of the Power Spectral Density (PSD). Therefore, the signals were filtered using a bandpass with cut-off frequencies at $1 - 40\,\mathrm{Hz}$ and automatically selected data sequences of 10 s were analyzed. Further details about the EEG monitoring and analysis procedures can be found elsewhere. [18]

Results and Discussion

Wettability Evaluation of the Plasma Treated PU Surfaces

The hydrophilicity of the untreated and Ar, O_2, and N_2 plasma treated polyurethane samples was evaluated as a function of the treatment parameters that were used, since it is a reliable indicator for the formation of reactive groups and surface roughness promotion, which is expected to promote the desired thin film adhesion levels. [55]

Figure 1a and b represent the water contact angle (C.A.) evolution with increasing plasma treatment times and powers for the three used gases, respectively. Regarding the plasma treatment time parameter, Figure 1a, all treatments were performed with a fixed power of 100 W (equipment maximum) and increasing exposure times from 2 to 20 min .

Figure 1 shows that it is possible to reduce the water C.A. from 90° (untreated) to $40 - 45°$ after only 2 min of activation (valid for all gases). Subsequently, with further increase of the plasma treatment time, a clear differentiation of the C.A. behavior is patent, taking

into account the different gases used. The most pronounced reduction of the C.A. is achieved using Ar, with a minimum of 12° after 15 min of exposure, corresponding to a hydrophilicity increase of 87%, comparing to the untreated value. When a 20 min treatment is performed, the water C.A. values suffer a slight increase until 21°. Regarding the nitrogen series, a constant decrease of the C.A. values can be seen up to 20 min of treatment time (minimum of 25°, 72% hydrophilicity increase). As for the oxygen treatments, a minimum C.A. of 42° is achieved after 5 min (53% hydrophilicity increase), with the values remaining rather constant with increasing activation times.

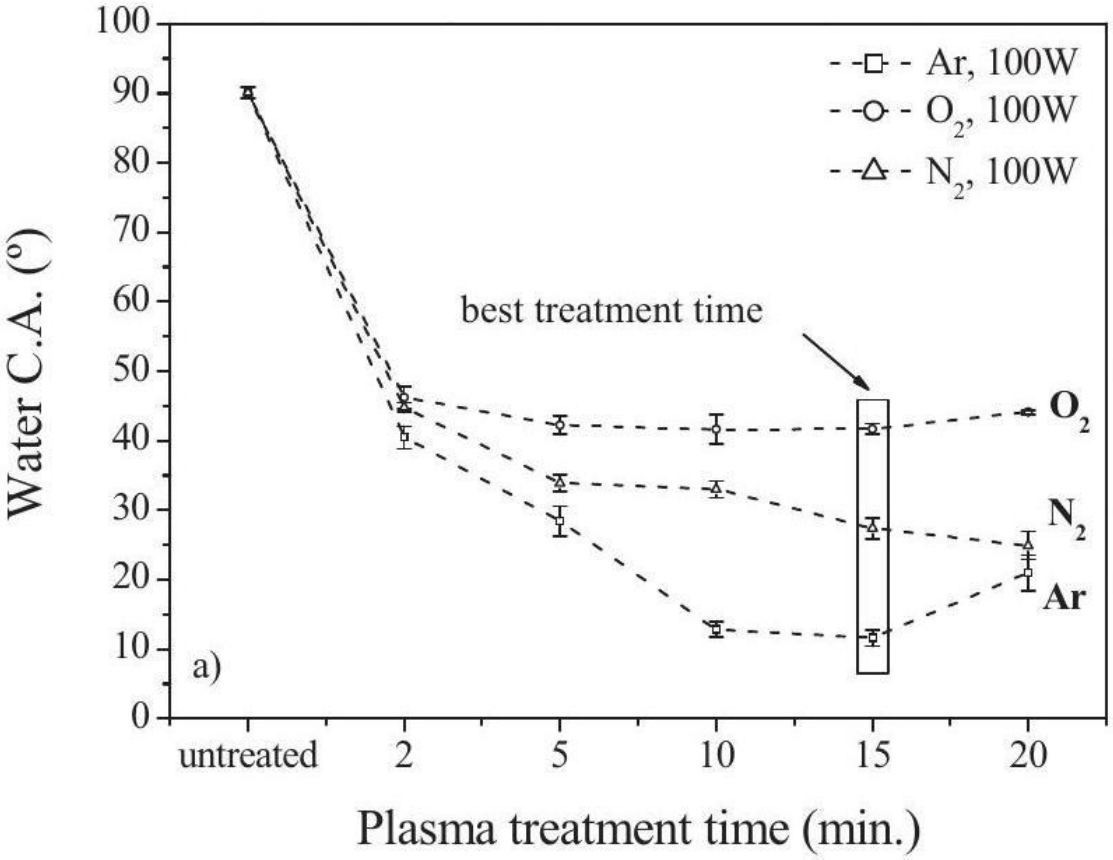
Water C.A. (°)
Plasma treatment time (min.)
Ar, 100W
O2, 100W
N2, 100W
best treatment time
O2
N2
Ar
a)
untreated
2
5
10
15
20

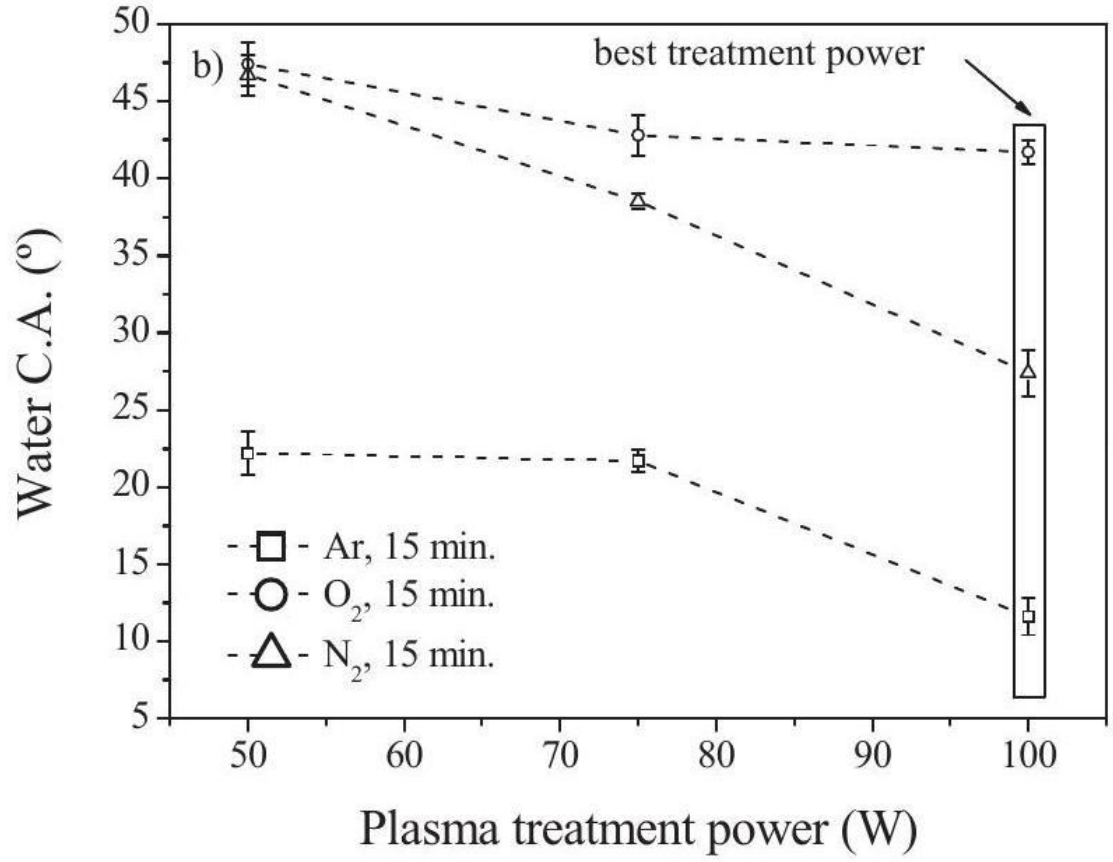
Water C.A. (°)
Plasma treatment power (W)
b)
best treatment power
Ar, 15 min.
O2, 15 min.
N2, 15 min.

Figure 1. Water contact angle evolution with (a) increasing plasma treatment times and with (b) decreasing plasma treatment power. Mean and standard error of the mean were calculated for all conditions (minimum of six measurements).

Taking into account the results of the exposure time variation in the water C.A., the 15 min plasma activation treatment was selected as the best treatment time, since all surfaces activated with the three used gases displayed the lowest C.A. value. In the case of the nitrogen activation, the slight decrease of the C.A. observed from 15 to 20 min was not considered as significant, taking into account that the error bars of both experimental data are overlaid. Hence, after selecting the most appropriate treatment time (15 min), the effect of the plasma power was also investigated by decreasing the values from 100 W (maximum power output allowed by the equipment used) to 50 W, Figure 1b. With the exception of the oxygen treatments (which display roughly the same C.A. with 100 and 75 W), the argon and nitrogen plasma ones exhibit increasing C.A. values with decreasing plasma powers. Consequently, regarding the water C.A. evolution, the plasma treatments that were found to be more effective in increasing the wettability/hydrophilicity of the PU surface were the ones performed with 100 W for 15 min , regardless of the used gas.

The water C.A. behavior of the plasma activated PU surfaces, consistent with results obtained by other authors, [29,35,39,48] may be explained by considering the Wenzel's equation [55,56]

$$\cos(\theta_W) = r\cos(\theta_Y) \quad (1)$$

Equation (1) describes the relation between the apparent C.A. on a rough surface (θ_W), the surface average roughness ratio (r , ratio between the real and geometric area) and the C.A. on a chemically similar smooth surface (θ_Y). Hence, taking into account this relation, it is possible to claim that the wettability evolution is strongly related with the chemical and topographic changes promoted by the plasma activation treatments. Therefore, an extensive surface chemical and topographical analysis will be performed in the subsequent sections of this work, in order to draw correlations regarding the observed water C.A. behavior.

Chemical Analysis of the Plasma Activated PU Surfaces

FTIR-ATR Analysis

The FTIR-ATR analysis was again performed on PU surfaces activated with different gases, exposure times, and plasma powers (same conditions as in the previous section) in order to validate the selection of the best plasma parameters (time and power) that were performed, taking into account the water C.A. behavior. However, unlike what was observed from the C.A. measurements, no significant changes could be seen when focusing on the exposure time and plasma power, with the respective spectra appearing overlaid. Hence, only the spectra that refer to the plasma conditions that originated the lowest water C.A. values (100 W , 15 min for all gases) are shown in Figure 2. Note that the exhibited spectra were shifted in relation to the baseline, in order to allow a better visualization of the peaks.

The bands at 3320 and 2956 cm^{-1} refer to N-H and C-H stretching (s), respectively. As for the peaks detected between 2000 and 1500 cm^{-1}, that may be indexed to $C = O$(s) at 1700 cm^{-1}, $C = C$(s) at 1600 cm^{-1} and $N - H$ bending (b) at 1528 cm^{-1}. From 1500 to 1000 cm^{-1}, the $C - H$ (b) at 1414 cm^{-1}, $-CH3$ (b) at 1312 cm^{-1}, $C - O$ (s) at 1216 cm^{-1} and C-O-C (s) at 1067 cm^{-1} bonds were observed. All the FTIR spectra were indexed according to references. [57,58]

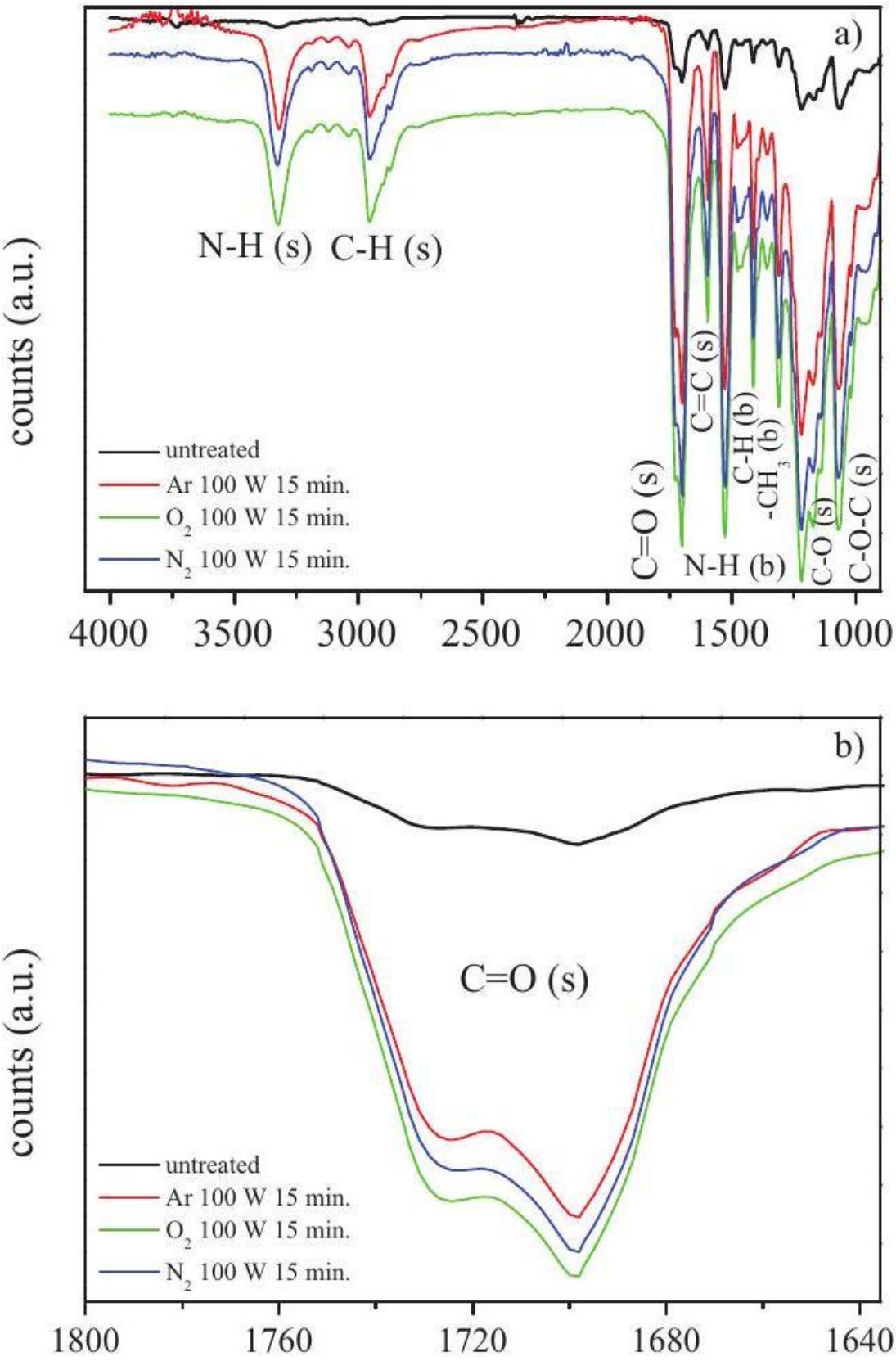
a)
counts (a.u.)
N-H (s)
C-H (s)
C=O (s)
C=C (s)
C-H (b)
-CH3 (b)
N-H (b)
C-O (s)
C-O-C (s)
untreated
Ar 100 W 15 min.
O2 100 W 15 min.
N2 100 W 15 min.
4000
3500
3000
2500
2000
1500
1000
b)
counts (a.u.)
C=O (s)
untreated
Ar 100 W 15 min.
O2 100 W 15 min.
N2 100 W 15 min.
1800
1760
1720
1680
1640
c)

Figure 2. FTIR spectra of the polyurethane samples (a) treated with the best treatment time and power for the three used gases. (b) and (c) represent magnifications of the reactive oxygen containing bonds. The signals were shifted in relation to the baseline in order to allow a better understanding of the promoted changes.

Major changes regarding the intensity of the indexed bands can be seen on the FTIR spectra of the activated surfaces when comparing to the untreated sample, meaning that the performed plasma treatments effectively changed the chemical surface of the PU samples, by increasing its reactivity (higher intensity of the reactive oxygen-containing groups can be seen). However, no new species were detected, regardless of the used gas, exposure time and plasma power, which was somewhat expected since FTIR is known for not being particularly sensitive to small amounts of chemical species. [55]

As the inclusion of reactive species is an important indicator of good polymer/thin film interfacial adhesion levels and may also explain the water C.A. evolution (bearing in mind the Wenzel's equation), the effect of the performed surface activation on the promotion of $C=O$, $C-O$, and $C-O-C$ bonds is shown on Figure 2 b and c . Despite the small intensity differences that are, once more, perceivable, the same behavior is patent when taking into account the changes promoted by the three gases. As expected, the Ar 100 W 15 min treatment consistently gives rise to lower amounts of oxygen-containing reactive species, due to the fact that argon is a non-reactive, ideal gas.

Hence, argon should mainly promote the formation of free radicals (dangling bonds) that may later recombine with oxygen and other elements (including water) when exposed to ambient air. [35,55] It is important to note that the activated PU samples were analyzed shortly after the plasma treatments, thus only a very brief exposure to ambient air occurred. In opposition, the treatments performed with nitrogen and, especially, oxygen are more effective in creating further amounts of reactive groups. Nitrogen, despite not being a noble gas, acts in a similar way to argon, by promoting the formation of free radicals due to the occurrence of extensive polymer chain scission. [29,30] The reactive groups are then formed by combination with ambient oxygen. When using oxygen as working gas, the reactive oxygen-containing functionalities are obtained during the plasma treatment itself. [35] Furthermore, some free radicals may also be formed and later recombine with the elements present in ambient air.

In conclusion, due to the lower water C.A. values already observed and beneficial inclusion of reactive species, the Ar100 W15 min, $O_2$100 W15 min and N_2 100 W 15 min plasma treatments were selected to be further investigated.

XPS Analysis

As the FTIR investigation was not sufficient to clearly differentiate the chemical effects of the used working gases, an extensive XPS analysis was performed on the PU surfaces activated with the previously optimized plasma conditions, Figure 3. The identification of the peaks was performed using references. [30,59]

From the XPS spectra analysis, it is possible to see significant changes when comparing the untreated and plasma treated samples, namely regarding the C1s signal (N1s and O1s spectra are not shown since no significant changes were found). It is important to note that some contaminations (F, Na, S, Cl, K, and Ca) were detected (peaks identified as * in

Figure 3). These contaminations were

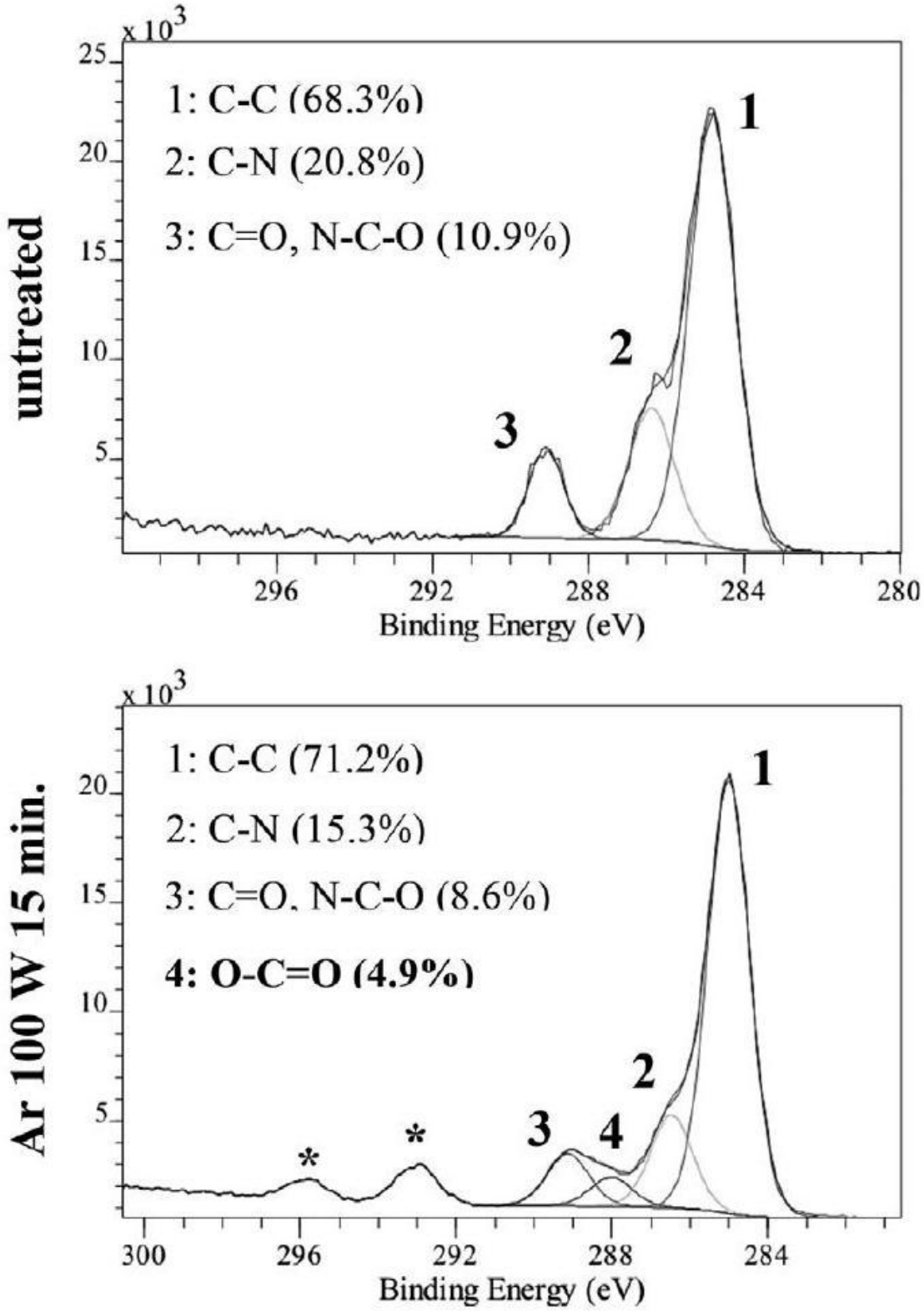
C1s
untreated
x 10^3
25
20
15
10
5
1: C-C (68.3%)
2: C-N (20.8%)
3: C=O, N-C-O (10.9%)
1
2
3
296
292
288
284
280
Binding Energy (eV)
Ar 100 W 15 min.
x 10^3
20
15
10
5
1: C-C (71.2%)
2: C-N (15.3%)
3: C=O, N-C-O (8.6%)
4: O-C=O (4.9%)
1
2
3
4
*
*
300
296
292
288
284
Binding Energy (eV)
x 10^3
20
18
16
1: C-C (62.4%)
2: C-N (21.5%)
1

Figure 3. XPS spectra (C1s signal only) of the untreated and plasma treated polyurethane substrates. * refers to impurities found in the bulk polymer. probably introduced in the manufacturing of the PU samples, as the related peaks were not reduced after ionic etching. This should mean that the impurities are part of the bulk polymer and not promoted by the plasma treatments.

All plasma treatments promoted the increase of the oxygen-containing functionalities (13.5, 16.1, and 15.9% for the Ar, O_2, and N_2 treatments, respectively), when comparing to the untreated PU sample (10.9%) in the C1s spectra. These results are consistent with the FTIR analysis performed in the previous section. Moreover, the insertion of a new chemical functionality at around 288 eV is perceivable due to the formation of $C = O$ or $N - C - O$ bonds at the surface of all activated PU samples. Note that in the FTIR analysis, no new reactive groups were detected after the performed plasma treatments. Despite not being reactive gases, the XPS analysis proves that argon and nitrogen are effective (although not in the same extent as oxygen) in promoting the desired chemical changes, including the creation of new functionalities, which should be mainly due to the higher ability to induce the formation of free radicals that later act as anchoring points for the oxygen species present in the ambient air. Oxygen is then the most effective working gas regarding the production of reactive groups. The grafting of such reactive oxygen-containing groups should, in fact, be responsible for the increased hydrophilicity of the activated samples.

Nevertheless, this set of results seem to indicate that the chemical alterations studied by FTIR and XPS do not provide a clear explanation for the wettability differences that were promoted by the different working gases. As previously seen, the Ar 100 W 15 min plasma treatment promoted lower water C.A. values (12°) than the $N_2$100 W 15 min(25°) and $O_2$100 W15 min(42°) ones, despite being less effective in the chemical functionalization of the PU surfaces. It is also important to note that the argon treatment promoted the least amount of oxygencontaining groups (13.5%), followed by nitrogen (15.9%) and finally oxygen (16.1%). Hence, considering only the surface chemical chances, no definitive explanations can be found regarding the observed water C.A. behavior. Consequently, taking into account equation (1), the wettability behavior should be further explained by investigating the topography changes induced on the activated PU surfaces.

Topographic Features of the Plasma Treated PU Samples

Wenzel's equation shows that for a hydrophilic surface ($\theta_Y < 90°$) the roughness should turn the surface more hydrophilic and a hydrophobic surface ($\theta_Y > 90°$) more hydrophobic. However, for water C.A. close to 90° this parameter is insensitive to roughness variations. In addition, the more hydrophilic the surface is, the higher the effect of the roughness on the water C.A. It was seen that the water C.A. of the PU substrates decreased from 90° (untreated) to a minimum of 42,25 , and 12° for the $O_2$100 W15 min, N_2 100 W 15 min, and Ar 100 W 15 min plasma treatments, respectively. These wettability variations from the untreated to the plasma treated polymer can be explained, in part, by the significant grafting of oxygen-containing species in the surface of the activated PU samples. However, as seen in the previous section, the chemical changes are not able to explain the hydrophilicity changes observed for the different working gases, as the sample treated

with the gas that promoted the formation of higher amounts

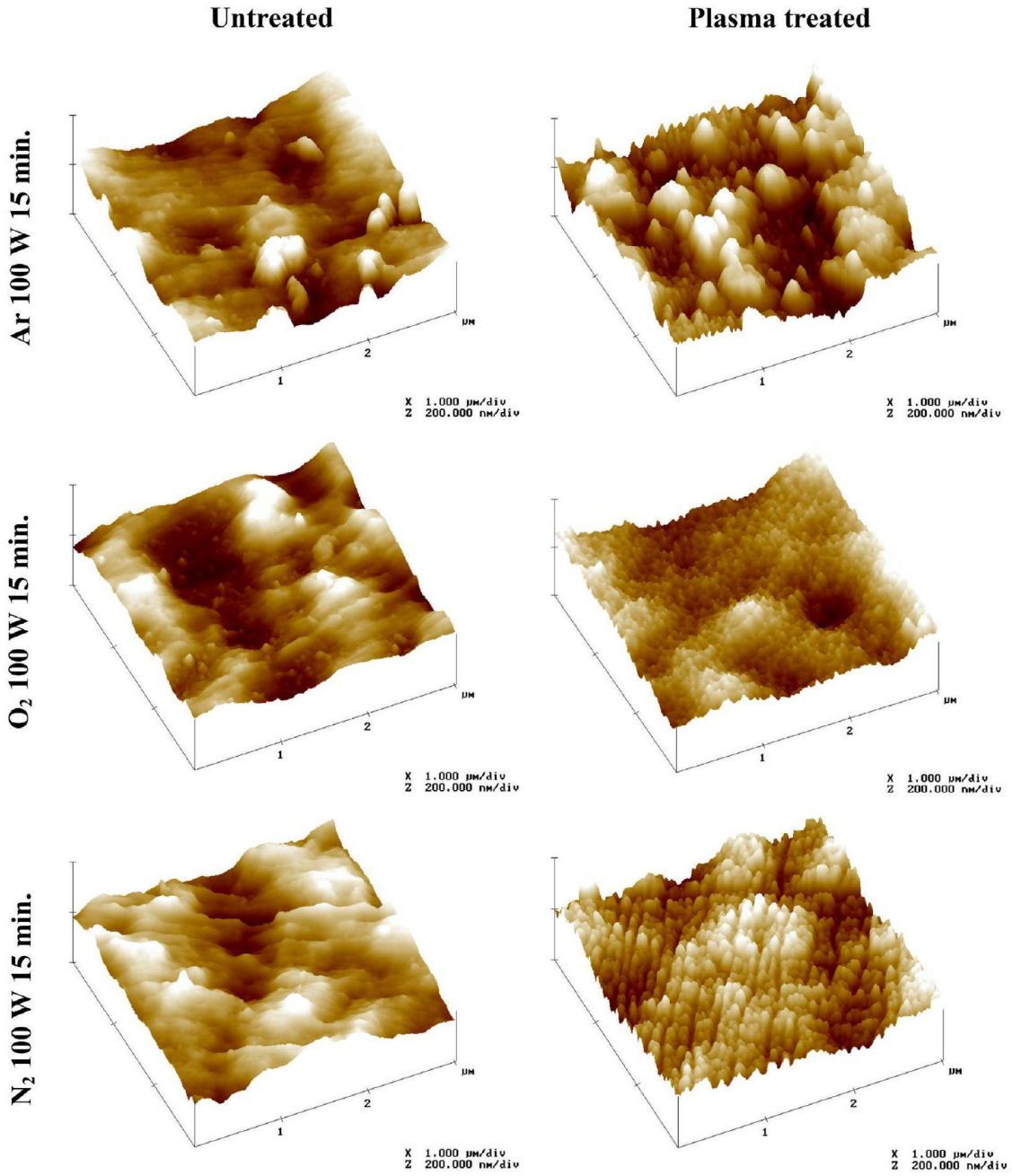

of reactive oxygen-containing groups (oxygen, 16.1%) displayed the higher water C.A. (42°). In opposition, the Ar treatment exhibited the lowest water C.A. (12°) despite promoting the formation of less amounts of reactive species (13.5%).

Hence, the wettability behavior should be further explained by the topographic changes promoted by the different plasma treatments, Figure 4. In order to take account of potential irreproducibility in the fabrication of the PU samples that may derive from the manufacturing process (compression molding), three untreated samples were selected, suitably identified and then, activated with the selected conditions and working gases.

Once more, clear topographic differences can be seen when comparing the plasma treated PU surfaces to their untreated counterparts. Furthermore, the different topographic effects promoted by each of the working gases are also clear. Finer topographic features seem to be introduced by the nitrogen and oxygen treatments, while argon promotes the formation of a coarser topography. Looking at Table 3, it is possible to see that the Ar 100 W 15 min treatment gives rise to the highest increase of the average roughness of the PU surfaces, increasing from 19.3 nm (untreated) to 37.8 nm .

The average roughness of the untreated sample was then almost doubled (96% increase) when using argon as working gas. In opposition, the oxygen treatment promotes the least amount of topographic changes, with the average roughness increasing from 16.4 nm (untreated sample) to 21.6 nm , meaning that only a 31% increase of the surface roughness was achieved. The $N_2$100 W15 min activation originates intermediate changes of the surface topography, with the roughness suffering a 48% increase, from 19.5 nm to 28.9 nm . It is interesting to note that all plasma treatments gave rise to increased surface roughness of the PU samples. These results are not consistent with the work of other authors, [35] where a softening of the surface was observed, which must be due to the lower activation times that were used (3 min vs. 15 min). Hence, it is possible to say that higher plasma activation times are beneficial for the promotion of increased surface roughness on PU samples.

To summarize, regarding the influence of the chemical changes and surface roughness promotion on the wettability behavior of the PU samples, a clear relation is perceivable. The samples treated with argon, which display the highest roughness increase (96%), are also more hydrophilic (lower water C.A., 12°), despite also exhibiting the lowest amount of reactive oxygen-containing groups (13.5%). In turn, the PU samples activated using oxygen as working gas, which present the most chemically active surface (grafting of 16.1% of reactive species), display the least amount of topographic changes (31% roughness increase) and the highest water C.A. value (42°). The samples activated with the $N_2$100 W15 min plasma treatment exhibit intermediate water C.A. values (25°), which should be due to the also intermediate roughness increase (48%) and grafting of oxygen reactive groups (15.9%).

In conclusion, all plasma treatments performed with the optimized conditions (100 W, 15 min) are effective in producing the desired wettability changes, through the grafting of reactive oxygen-containing species and roughness promotion on the surface of the PU samples. The extent of the aforementioned surface alterations is dependent on the used working gas and the hydrophilicity behavior is effectively explained by taking into consideration the relation between chemical and topographic changes patent in the Wenzel's equation (1).

PU/Ag:TiN Adhesion Assessment

In order to investigate if the performed plasma treatments promote, in fact, an enhancement of the PU/thin film interfacial adhesion, a Ag:TiN coating (with N/Ti atomic ratio of 0.7 and 6 at. %Ag; thickness of ~ 600 nm) was deposited on the untreated and plasma treated PU substrates. The adhesion was studied using the cross-cut tape test, according to the ASTM D3359-B standard (which provides a decreasing adhesion classification between 5B and OB) and the results are patent in Figure 5.

As expected, due to the significant chemical and topographic changes underwent by the plasma treated PU surfaces (grafting of reactive oxygen-containing

Table 3. Roughness variation promoted by the performed plasma treatments. Mean and standard error of the mean were calculated for all conditions (3 repetitions).

	Untreated		Plasma treated		
Plasma treatment	R_a(nm)	RMS (nm)	R_a(nm)	RMS (nm)	ΔR_a (%)
Ar 100 W 15 min	19.3 ± 1.1	24.5 ± 1.4	37.8 ± 1.1	46.6 ± 2.3	+96
$O_2$100 W15 min	16.4 ± 1.3	20.9 ± 0.8	21.6 ± 1.4	27.2 ± 1.7	+31
$N_2$100 W15 min	19.5 ± 1.6	24.6 ± 1.7	28.9 ± 2.7	35.2 ± 3.3	+48

untreated
4 mm
500 µm
Ar 100 W 15 min.
4 mm
500 µm
O2 100 W 15 min.
4 mm
500 µm
N2 100 W 15 min.
4 mm
500 µm

Figure 5. SEM imaging of the cross-cut tape tests performed on the untreated and plasma treated Ag:TiN-coated polyurethane substrates.
aforementioned standard, the appropriate adhesion classification seems to be 3B: small flakes of the coating are detached along the edges and at the intersections of the cuts; the area affected is 5 to 15% of the lattice. In opposition, no definitive differences can be found among the plasma treated samples. However, the argon treated sample seems to exhibit slightly higher amounts of cracks, which may be an indication of the importance of the grafting of reactive oxygen-containing groups. Note that the argon treatment promoted the formation of smaller amounts of reactive species (13.5%). All plasma treatments, Ar 100 W 15 min, O_2 100 W 15 min, and N_2 100 W 15 min , translate into excellent levels of interfacial adhesion (rated as 5B - the edges of the cuts are completely smooth; none of the squares of the lattice is detached), as no delamination is perceivable. All chemical and topographic combined results seem to indicate that the key parameter controlling the interfacial adhesion should be the grafting of reactive chemical groups and not the observed roughness changes.

Hence, it is possible to conclude that the performed plasma treatments produced the desired increase of the PU/Ag:TiN interfacial adhesion by effectively activating the PU surface chemically and by increasing the surface roughness. Both parameters should lead to an increase of anchoring and interlocking points to the sputtered Ag:TiN film. [55]

EEG Trials

With the objective of investigating if the proposed technological approach was suitable to be used as EEG electrodes, three sets of PU MP electrodes were activated using the previously optimized plasma conditions and subsequently coated with the same Ag:TiN coating used in the previous section. As the non-treated PU flat samples did not display an acceptable coating/substrate adhesion performance, exhibiting strongly delaminated areas (a phenomenon that would be even more relevant in the coating of complex substrate designs) - only the plasma treated conditions substrate designs) - only the plasma treated conditions
species and increase of the surface roughness), the untreated sample exhibits the lowest adhesion to the Ag:TiN film. As it can be seen from the backscattered images, extensive delamination can be seen not only along the cuts, but also inside some of the squares (although in a smaller extent). According to the
a)

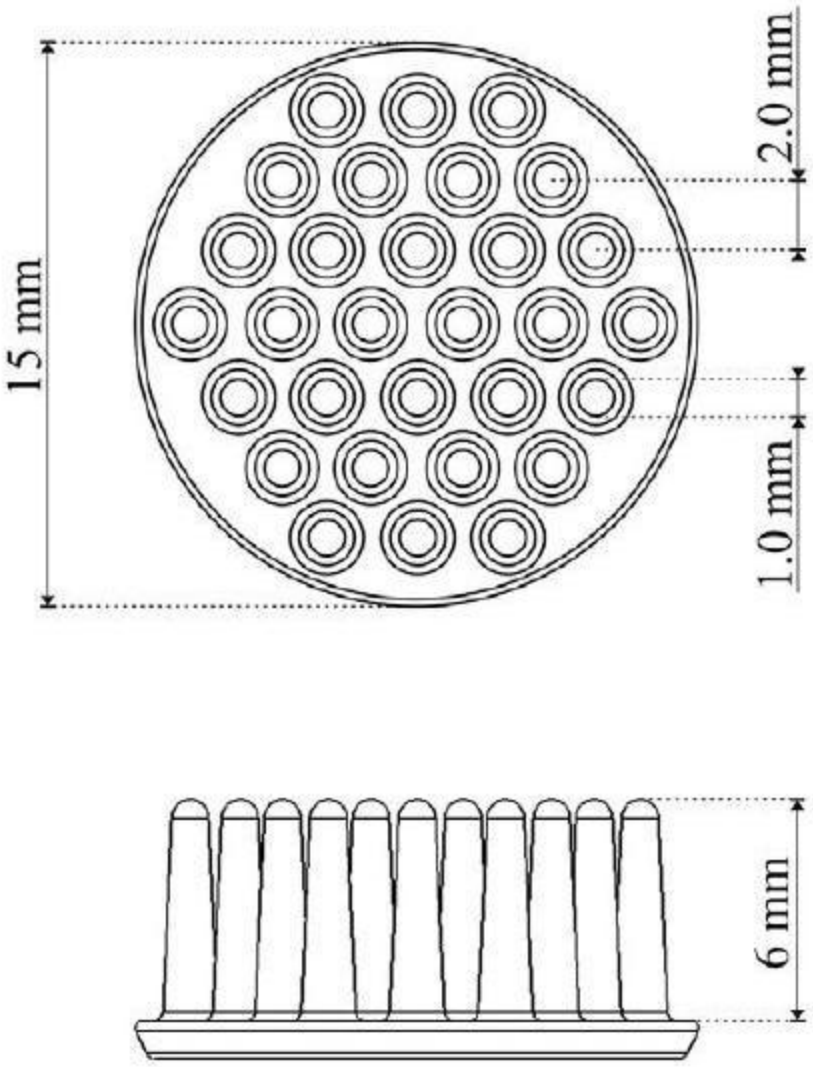

Figure 6. PU multipin electrode used for the EEG tests. (a) electrode design and (b) plasma activated Ag:TiN-coated electrode.
were selected for the coating of the PU MP electrodes, Figure 6.

Subsequently, the dry MP electrodes were used in parallel with the commercial wet Ag/AgCl electrodes in several EEG monitoring tests, in order to assess their characteristics in a realistic EEG acquisition scenario and to evaluate if considerable signal differences could be found among the electrodes.

After determination of the RMSD (root mean square deviation) and CORR (Spearman's rank correlation) values for each plasma activated and reference electrodes (3 subjects, 3 repetitions) separately, the mean and the standard deviation over all subjects and test repetitions was calculated. The resulting values are listed in Table 4. As it is possible to see, the magnitude of the calculated RMSDs of the plasma activated and Ag:TiN-coated polyurethane MP dry electrodes is only marginally lower (maximum difference of 2.4μ V) than the RMSD of the wet Ag/AgCl reference test.

Similar trends are visible for the VEP results (maximum difference of 0.9μ V) and the Spearman's rank correlation. These negligible differences between the

b)

monitored EEG signals are likely caused by the spatial distance of the two occipital electrode positions, as well as environmental noise or even due to inevitable experimental differences that derive from the manual positioning and preparation of the electrodes. [15,17,18] Moreover, taking into account the high correlation values (>0.8) as well as the standard deviations (for both RMSD and CORR), no considerable differences in terms of signal quality can be identified: neither (i) between dry MP and wet electrodes, nor (ii) among the different dry MP electrodes. Furthermore, no considerable alterations of the shape and amplitude of the EEG signals can be seen, regardless of the used electrode, Figures 7 and 8.

Hence, data from Table IV, Figure 7 and 8 indicate that the relevant EEG signal information can be recorded with both the proposed plasma activated and Ag:TiN-coated polyurethane MP dry electrodes and the reference conventional wet Ag/AgCl electrodes.

In order to analyze frequency-dependent signal differences, the mean power spectral density (PSD) of the EEG signals was calculated over all subjects and test repetitions and is shown in Figure 9 for the wet reference and the dry test signals. Resting state EEG and alpha activity (Figure 9a and b, respectively) show similar trends. The power increases for lower frequencies for all electrodes. For frequencies below 3 Hz , an increase toward higher values is perceivable in the plasma treated dry MP electrodes, which should be attributed to slightly increased drift behavior, which was already observed in previous studies. [17]

To summarize, the small differences found in terms of EEG signal characteristics, shape and amplitude indicate that the proposed dry MP electrodes are promising candidates to replace the standard wet Ag/AgCl ones,

Table 4. Signal differences between the plasma treated Ag:TiN-coated polyurethane MP dry electrodes vs. Ag/AgCl reference wet electrodes calculated for the VEP, as well as for 10 s long sequences of resting state EEG, alpha activity, and EEG containing eye blink artefacts. Mean and standard deviation calculated over all subjects and repetitions.

Plasma treatment	RMSD (μV)				CORR			
	Resting	Alpha	Eye blink	VEP	Resting	Alpha	Eye blink	VEP
Ar 100 W 15 min	8.3 ± 2.9	7.5 ± 2.6	7.9 ± 1.9	0.5 ± 0.08	0.85 ± 0.15	0.86 ± 0.18	0.94 ± 0.06	0.97 ± 0.01
$O_2$100 W15 mi	6.9 ± 3.7	6.5 ± 2.5	6.5 ± 1.6	0.6 ± 0.06	0.81 ± 0.20	0.82 ± 0.17	0.97 ± 0.07	0.97 ± 0.01
$N_2$100 W15 mi	7.4 ± 2.6	7.3 ± 2.0	7.4 ± 1.3	0.9 ± 0.09	0.83 ± 0.12	0.86 ± 0.13	0.96 ± 0.08	0.97 ± 0.01
Ag/AgC reference	5.9 ± 2.0	6.0 ± 1.6	6.2 ± 0.9	0.5 ± 0.1	0.88 ± 0.12	0.89 ± 0.09	0.98 ± 0.04	0.97 ± 0.01

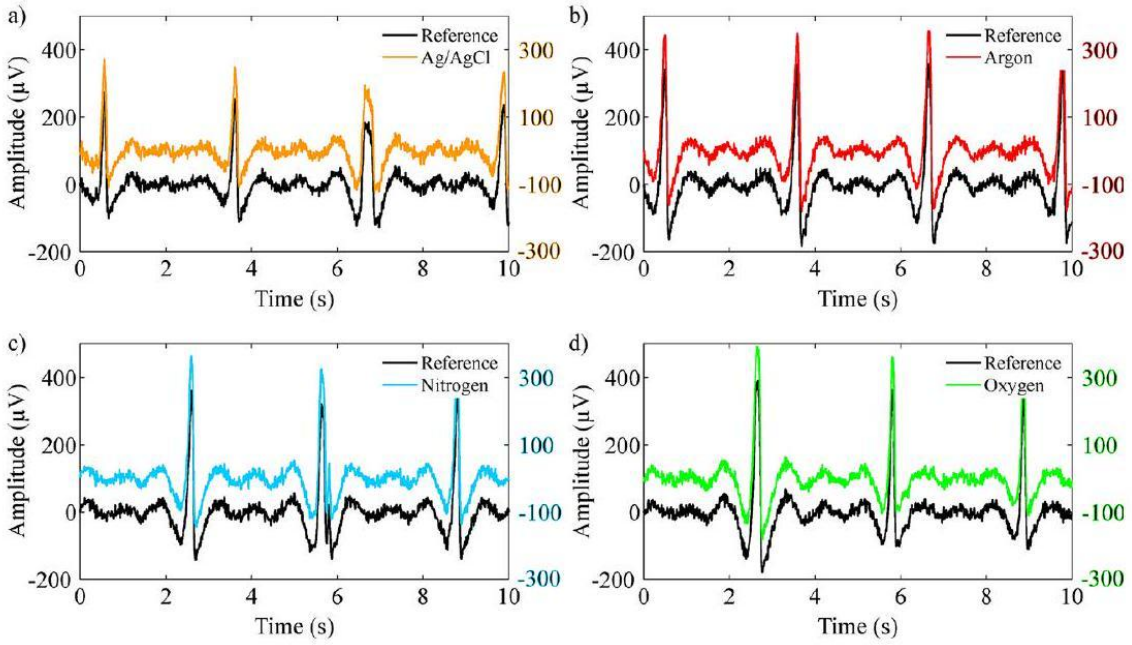

Figure 7. Overlay plot of 10 s of EEG signal containing eye-blinking artefacts recorded with (a) two independent wet Ag/AgCl reference electrodes, (b) Ag/AgCl reference & Ar treated MP dry electrode, (c) Ag/AgCl reference &N_2 treated MP dry electrode, and (d) Ag/AgCl reference & O_2 treated MP dry electrode pairs.

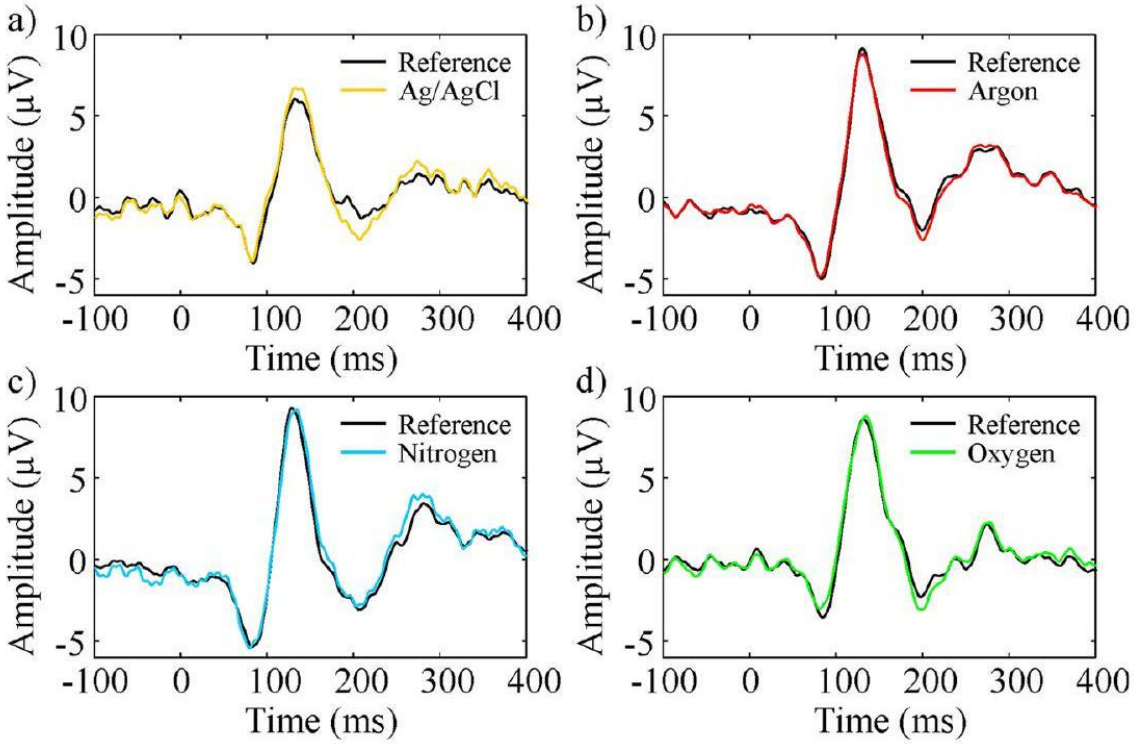

Figure 8. Overlay plot of the VEP results 100 ms pre- and 400 ms post-stimulus acquired with (a) two independent wet Ag/AgCl reference electrodes, (b) Ag/AgCl reference & Ar treated MP dry electrode, (c) Ag/AgCl reference & N_2 treated MP dry electrode, and (d) Ag/AgCl reference & O_2 treated MP dry electrode pairs. which should translate into faster and simple montages, beneficial for many clinical or ambulatory procedures.

Conclusion

The present study focused on the optimization of the plasma treatment conditions with the objective of enhancing the PU/Ag:TiN system interfacial adhesion so that it may be later used as dry EEG electrodes. The optimal treatment conditions were selected taking into account the influence of the exposure time and plasma power on the wettability of the PU surfaces. Minimum water C.A. values (42, 25, and 12° for oxygen, nitrogen and argon, respectively) were obtained using 100 W and 15 min , regardless of the used working gas. The steep reduction from 90° (untreated PU) was attained due to significant chemical and topographic changes of the PU surface. After FTIR and XPS analysis it was found that the plasma activation promoted the grafting of reactive oxygen-containing groups at the PU surface. Oxygen was the most effective gas, inducing the formation of higher amounts of the referred species (16.1%), followed by nitrogen (15.9%) and argon (13.5%). Furthermore, the Wenzel's equation predicted that also topography changes should play an important role on the hydrophilicity evolution, thus from the AFM studies it was found that a 96, 48, and 31% roughness increase was promoted by the argon, nitrogen, and oxygen, respectively. As expected, the promoted chemical and topographic changes translated into an excellent PU/Ag:TiN interfacial adhesion, being rated with the maximum classification of 5B. The untreated PU sample exhibited extensive delamination

along the edges of the cuts and in some areas inside the squares defined by the crosscut tape test.

The results obtained from the EEG trials allowed to conclude that no considerable differences in terms of shape, amplitude, and spectral characteristics were found when comparing signals acquired by conventional wet reference Ag/AgCl electrodes and the proposed plasma activated and Ag:TiNcoated polyurethane dry MP electrode, regardless of the used plasma working gas. No differences between the dry electrodes themselves could also be found. Consequently, since most of the EEG signal information is maintained when the dry electrode system proposed in the present work is used, it is possible to conclude that the PU/Ag:TiN dry electrodes are promising candidates to substitute the standard Ag/AgCl ones in specific clinical and ambulatory procedures.

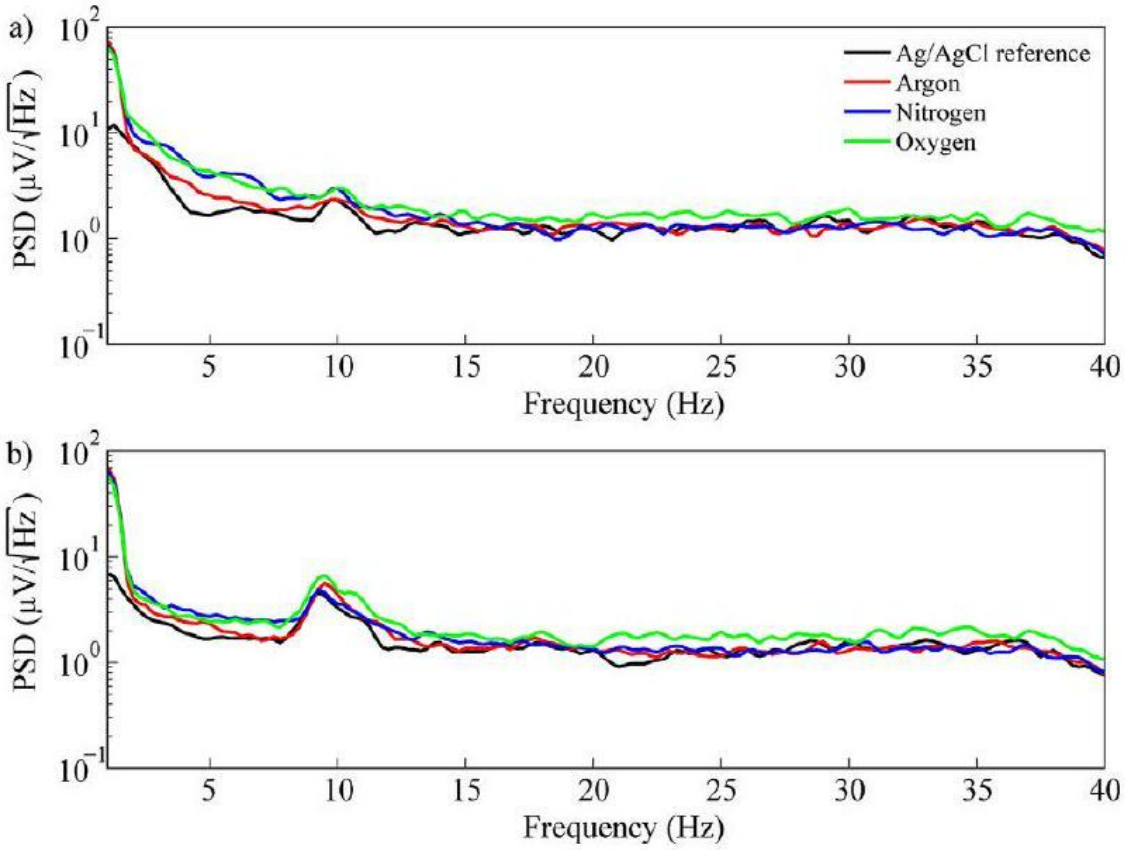

Figure 9. Characteristic EEG signals acquired with the proposed plasma treated Ag: TiN-coated polyurethane MP dry electrodes and conventional Ag/AgCl electrodes: Welch estimation of the mean power spectral density of 10 s of (a) resting state EEG and (b) EEG exhibiting alpha activity calculated over all subjects and test repetitions.

Acknowledgments: This research is partially sponsored by FEDER funds through the program COMPETE - Programa Operacional Factores de Competitividade and by national funds through FCT Fundação para a Ciência e a Tecnologia, under the projects PEst-C/EME/UI0285/2011, PTDC/SAU-ENB/116850/2010, PTDC/CTMNAN/112574/2009, and Programa Pessoa 2012/2013 Cooperação Portugal/França, project no. 27306UA Porous architectures in GRAded CERamic thin films for biosensors - GRACER. The

authors would also like to acknowledge CEMUP for SEM analysis and Yantai Wanhua Polyurethanes Co., Ltd for providing the thermoplastic polyurethane pellets. P. Pedrosa acknowledges FCT for the Ph.D. grant SFRH/BD/70035/2010. P. Fiedler acknowledges the German Federal Ministry of Education and Research project 03IPT605A. P. Pedrosa and P. Fiedler both acknowledge FP7-People Marie Curie IAPP project 610950 (ANDREA) and German Academic Exchange Services for the Germany/Portugal bi-lateral project - D/ 57036536.

Keywords: Ag-doping; dry electrodes; EEG; interfacial adhesion; plasma activation

[1] M. Teplan, Meas. Sci. Rev. 2002, 2, 1.
[2] E. McAdams, "Bioelectrodes", in Encyclopaedia of Medical Devices and Instrumentation, J. G. Webster, Ed., Wiley, New York 1988, p. 120-166.
[3] A. Searle, L. Kirkup, Physiol. Meas. 2000, 22, 271.
[4] T. H. Sander, T. R. Knösche, A. Schlögl, F. Kohl, C. H. Wolters, J. Haueisen, L. Trahms, Biomed. Tech. 2010, 55, 65.
[5] P. Fiedler, S. Griebel, P. Pedrosa, C. Fonseca, F. Vaz, L. Zentner, F. Zanow, J. Haueisen, Sensor Actuat.: A Phys. 2014, 139.
[6] Z. Iscan, Z. Dokur, Biomed. Signal Proces. 2014, 10, 145.
[7] F. Akram, H.-S. Han, T.-S. Kim, Comput. Biol. Med. 2014, 45, 118.
[8] L.-D. Liao, C.-T. Lin, K. McDowell, A. E. Wickenden, K. Gramann, T.-P. Jung, L.-W. Ko, J.-Y. Chang, Pr. Inst. Electr. Elect. 2012, 100, 1553.
[9] B. A. -Taheri, R. T. Knight, R. L. Smith, Electroen. Clin. Neuro 1994, 90, 376.
[10] P. Brunner, L. Bianchi, C. Guger, F. Cincotti, G. Schalk, J. Neural Eng. 2011, 8, 025001.
[11] E. S. Valchinov, N. E. Pallikarakis, Biomed. Eng. OnLine 2004, 3, 25.
[12] C. Fonseca, J. P. Silva Cunha, R. E. Martins, V. Ferreira, J. P. Marques de Sá, M. A. Barbosa, A. Martins Silva, IEEE Trans. Biomed. Eng. 2007, 54, 162.
[13] B. A. -Taheri, R. T. Knight, R. L. Smith, Sens. Actuat. A 1996, 54, 606.
[14] N. S. Dias, J. P. Carmo, A. F. da Silva, P. M. Mendes, J. H. Correia, Sens. Actuat. A 2010, 164, 28.
[15] P. Fiedler, L. T. Cunha, P. Pedrosa, S. Brodkorb, C. Fonseca, F. Vaz, J. Haueisen, Meas. Sci. Technol. 2011, 22, 124007.
[16] P. Pedrosa, E. Alves, N. P. Barradas, P. Fiedler, J. Haueisen, F. Vaz, C. Fonseca, Corros. Sci. 2012, 56, 49.
[17] P. Fiedler, P. Pedrosa, S. Griebel, C. Fonseca, F. Vaz, F. Zanow, J. Haueisen, "Novel Flexible Dry PU/TiN-Multipin Electrodes: First Application in EEG Measurements". Proceedings of the 33rd Annual International Conference of the IEEE EMBS 2011, pp. 55-58.
[18] P. Fiedler, P. Pedrosa, S. Griebel, C. Fonseca, F. Vaz, E. Supriyanto, F. Zanow, J. Haueisen, Brain Topo. 2015, in print. DOI: 10.1007/s10548-015-0435-5
[19] Y. M. Chi, Y.-T. Wang, Y. Wang, C. Maier, T.-P. Jung, G. Cauwenberghs, IEEE Trans. Neural Syst. Rehabil. Eng. 2012, 20, 228.
[20] P. Fiedler, J. Haueisen, D. Jannek, S. Griebel, L. Zentner, F. Vaz, C. Fonseca, Acta IMEKO 2014, 3, 33.
[21] V. Marozas, A. Petrenas, S. Daukantas, J. Electrocardiol. 2011, 44, 189.
[22] G. Gargiulo, R. A. Calvo, P. Bifulco, M. Cesarelli, C. Jin, A. Mohamed, A. Van Schaik,

Clin. Neurophysiol. 2010, 121, 686.
[23] K.-P. Hoffmann, R. Ruff, "Flexible Dry Surface-electrodes for ECG Long-term Monitoring", Proceedings of the 29th Annual International Conference of the IEEE EMBS, Lyon, France, August 2007, p. 23-26.
[24] J. Baek, J. An, J. Choi, K. Park, S. Lee, Sens. Actuators A 2008, 143, 423.
[25] A. Gruetzmann, S. Hansen, J. Muller, Physiol. Meas. 2007, 28, 1375.
[26] R. J. Zdrahala, I. J. Zdrahala, J. Biomater. Appl. 1999, 14, 67.
[27] K. Stokes, A. Coury, P. Urbanski, J. Biomater. Appl. 1986, 1, 411.
[28] A. Tiwari, H. Salacinski, A. M. Seifalian, G. Hamilton, Cardiovasc. Surg. 2002, 10, 191.
[29] M. R. Sanchis, O. Calvo, O. Fenollar, D. Garcia, R. Balart, Polymer Testing 2008, 27, 75.
[30] C. Zandén, M. Voinova, J. Gold, D. Mörsdorf, I. Bernhardt, J. Liu, Eur. Polym. J. 2012, 48, 472.
[31] P. Pedrosa, D. Machado, C. Lopes, E. Alves, N. P. Barradas, N. Martin, F. Macedo, C. Fonseca, F. Vaz, Appl. Surf. Sci. 2013, 285P, 40.
[32] P. Pedrosa, E. Alves, N. P. Barradas, N. Martin, P. Fiedler, J. Haueisen, F. Vaz, C. Fonseca, Electrochim. Acta 2014, 125, 48.
[33] P. Pedrosa, D. Machado, M. Evaristo, A. Cavaleiro, C. Fonseca, F. Vaz, J. Vac. Sci. Technol. A 2014, 32, 031515.
[34] P. Pedrosa, C. Lopes, N. Martin, C. Fonseca, F. Vaz, Mater. Lett. 2014, 115, 136.
[35] P. Alves, S. Pinto, H. C. de Sousa, M. H. Gil, J. Appl. Polym. Sci. 2011, 122, 2302.
[36] N. Gomathi, A. Sureshkumar, S. Neogi, Curr. Sci. 2008, 94, 1478.
[37] P. Chu, J. Chen, L. Wang, N. Huang, Mater. Sci. Eng. R 2002, 36, 143.
[38] M. Noeske, J. Degenhardt, S. Strudthoff, U. Lommatzsch, Int. J. Adhes. 2004, 24, 171.
[39] Y. Ozdemir, N. Hasirci, K. Serbetci, J. Mater. Sci. Mater. Med. 2002, 13, 1147.
[40] T. Yamamoto, J. R. Newsome, D. S. Ensor, IEEE Trans. Ind. Appl. 1995, 31, 494.
[41] Y. Zhao, S. Tang, S.-W. Myung, N. Lu, H.-S. Choi, Polym. Test. 2006, 25, 327.
[42] I. Gancarz, G. Pozniak, M. Bryjak, Eur. Polym. J. 2000, 36, 1563.
[43] C. Oehr, Instr. Meth. Phys. Res. B 2003, 208, 40.
[44] D. Hegemann, H. Brunner, C. Oehr, Nucl. Instr. Meth. B 2003, 208, 281.
[45] E. M. Liston, L. Martinu, M. R. Wertheimer, J. Adhes. Sci 1993, 7, 1091.
[46] R. Molina, P. Erra, L. Julia, E. Bertran, Text. Res. J. 2003, 73, 955.
[47] Y. M. Chung, M. J. Jung, J. G. Han, M. W. Lee, Y. M. Kim, Thin Solid Films 2004, 447, 354.
[48] Y.-H. Li, Y.-D. Huang, Surf. Coat. Technol. 2007, 201, 5124.
[49] Y. Zhang, S. Myung, H. Choi, I. Kim, J. Choi, J. Ind. Eng. Chem. 2002, 8, 236.
[50] N. T. Correia, J. J. M. Ramos, B. J. V. Saramago, J. C. G. Calado, J. Colloid. Interf. Sci. 1997, 189, 361.
[51] E. Chibowski, Adv. Colloid. Interf. Sci. 2003, 103, 149.
[52] K. Rokosz, T. Hryniewicz, Adv. Mat. Sci. 2013, 13, 13.
[53] N. P. Barradas, C. Jeynes, R. P. Webb, Appl. Phys. Lett. 1997, 71, 291.
[54] A. F. Gurbich, Nucl. Instr. Meth. Phys. Res. Section B 2010, 268, 1703.
[55] P. Pedrosa, J.-M. Chappé, C. Fonseca, A. V. Machado, J. M. Nóbrega, F. Vaz, Plasma Process. Polym. 2010, 7, 676.
[56] G. Wolansky, A. Marmur, Colloids Surf. A 1999, 156, 381.
[57] L. Jiao, H. Xiao, Q. Wang, J. Sun, Polym. Degrad. Stab. 2013, 98, 2687.
[58] Y. Zhang, J. Maxted, A. Barber, C. Lowe, R. Smith, Polym. Degrad. Stab. 2013, 98, 527.
[59] X. Fu, M. J. Jenkins, G. Sun, I. Bertoti, H. Dong, Surf. Coat. Technol. 2012, 206, 4799.